

Organic & Biomolecular Chemistry

Accepted Manuscript



This is an *Accepted Manuscript*, which has been through the Royal Society of Chemistry peer review process and has been accepted for publication.

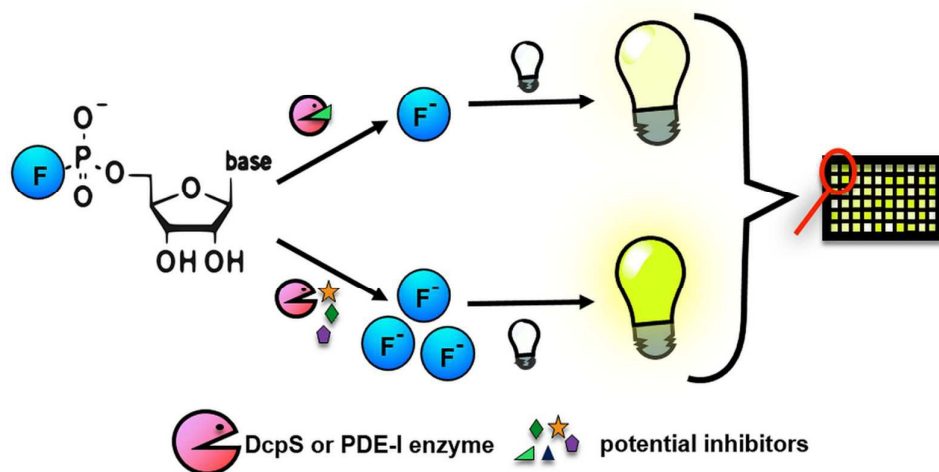
Accepted Manuscripts are published online shortly after acceptance, before technical editing, formatting and proof reading. Using this free service, authors can make their results available to the community, in citable form, before we publish the edited article. We will replace this *Accepted Manuscript* with the edited and formatted *Advance Article* as soon as it is available.

You can find more information about *Accepted Manuscripts* in the [Information for Authors](#).

Please note that technical editing may introduce minor changes to the text and/or graphics, which may alter content. The journal's standard [Terms & Conditions](#) and the [Ethical guidelines](#) still apply. In no event shall the Royal Society of Chemistry be held responsible for any errors or omissions in this *Accepted Manuscript* or any consequences arising from the use of any information it contains.

Fluorescent HTS assay for phosphohydrolases based on nucleoside 5'-fluorophosphates: application in screening for inhibitors of mRNA Decapping Scavenger and PDE-I

M. R. Baranowski^{a,†}, A. Nowicka^{a,b,†}, J. Jemielity^b and J. Kowalska^{a,*}



Several nucleotide-specific phosphohydrolases can cleave substrate analogues containing a fluorophosphate moiety to release fluoride ions. In this work, by employing a fluoride-sensitive probe, we harnessed this cleavage reaction to develop a fluorescence assay to screen for phosphohydrolase inhibitors.



Journal Name

ARTICLE

Fluorescent HTS assay for phosphohydrolases based on nucleoside 5'-fluorophosphates: application in screening for inhibitors of mRNA Decapping Scavenger and PDE-I

Received 00th January 20xx,
Accepted 00th January 20xx

DOI: 10.1039/x0xx00000x

www.rsc.org/

M. R. Baranowski^{a,†}, A. Nowicka^{a,b,†}, J. Jemielity^b and J. Kowalska^{a,*}

Several nucleotide-specific phosphohydrolases can cleave P-F bonds in substrate analogues containing a fluorophosphate moiety to release fluoride ions. In this work, by employing a fluoride-sensitive molecular sensor, we harnessed this cleavage reaction to develop a fluorescence assay to screen for phosphohydrolase inhibitors. The assay is rapid, sensitive, and based on simple and synthetically available reagents. The assay was adapted to the high-throughput screening (HTS) format and its utility was demonstrated by screening an 'in-house' library of small nucleotides against two enzymes: DcpS, a metal-independent mRNA decapping pyrophosphatase of the histidine triad (HIT) family; and PDE-I, a divalent cation-dependent nuclease. Our screening results agreed with the known specificities of DcpS and PDE-I, and led to selection of several inhibitors featuring low-micromolar IC₅₀ values. For DcpS, we also verified the results by using an alternative method with the natural substrate. Notably, the assay presented here is the first fluorescence-based HTS-adaptable assay for DcpS, an established therapeutic target for spinal muscular atrophy. The assay should be useful for phosphohydrolase specificity profiling and inhibitor discovery, particularly in the context of DcpS and other HIT-family enzymes, which play key roles in maintaining cellular functions and have been linked to disease development.

Introduction

Nucleotide-specific phosphohydrolases, including pyrophosphatases and nucleases, are enzymes that control the intracellular and extracellular levels of small nucleotides and thereby influence cellular metabolism, modulate signalling pathways,¹⁻³ and maintain the integrity of nucleic acids.⁴ In several cases, dysregulation of the activity of these enzymes has been linked to disease development, which indicates that these enzymes form a key class of therapeutic targets.^{5,6} Thus, numerous methods have been developed to quantify the activity of small-nucleotide-specific phosphohydrolases in vitro and in vivo and to evaluate potential inhibitors. These assays are commonly based on the use of radioactive probes or fluorescently labelled substrate analogues that exhibit 'turn-on' or 'turn-off' characteristics, or on the resolution of unlabelled substrates and products by using HPLC. However, the assays frequently suffer from one or more drawbacks, which limit their broad use and utility for high-throughput screening (HTS). For example, the radioactivity-based assays

require expensive radioscopically labelled probes and a dedicated experimental setup, the fluorescently labelled substrates generally require careful structure optimisation that involves laborious syntheses,⁷ and the HPLC method is both time-consuming and expensive. To overcome these drawbacks, researchers have continually sought to design novel assaying approaches. For example, several dual-labelled probes for producing the FRET effect or EPR measurements have been recently developed to monitor the activity of ATP and Ap_nA hydrolases.⁸⁻¹⁰ However, the cost of improved properties in the case of such probes is their high structural complexity, which necessitates low-yielding, multistep syntheses.

Nucleoside fluorophosphates are chemically stable and synthetically available nucleotide analogues.¹¹⁻¹⁴ We and others have previously shown that certain phosphohydrolases can cleave P-F bonds in nucleoside 5'-fluorophosphates (several HIT family members and PDE-I),^{13,15,16} 3'-fluorophosphates (PDE-II),¹⁷ and organophosphorus compounds (organophosphorus acid anhydrolase)¹⁸ to release a fluoride ion. Recently, we have demonstrated that this reaction can be used for monitoring the activity of pyrophosphatases by using ¹⁹F NMR.¹³ However, NMR experiments consume large amounts of reagents because their sensitivity is only moderate and high volumes of sample must be used, and the assays can be also hampered by the divalent metal cations required for catalytic activity. Therefore, in this work, we tested whether the fluoride release from nucleoside 5'-fluorophosphates can be quantified using a method that is

^a Division of Biophysics, Institute of Experimental Physics, Faculty of Physics, University of Warsaw, Zwirki i Wigury 93, 02-089 Warsaw, Poland. E-mail: asia@biogeo.uw.edu.pl

^b Centre of New Technologies, University of Warsaw, Banacha 2c, 02-097 Warsaw, Poland.

† These authors contributed equally to this work.

Electronic Supplementary Information (ESI) available: [details of any supplementary information available should be included here]. See DOI: 10.1039/x0xx00000x

more sensitive than ^{19}F NMR. Among numerous methods available for fluoride detection,¹⁹ we selected the use of a fluoride-sensitive fluorogenic probe, because this approach has previously been successfully employed to quantify fluoride

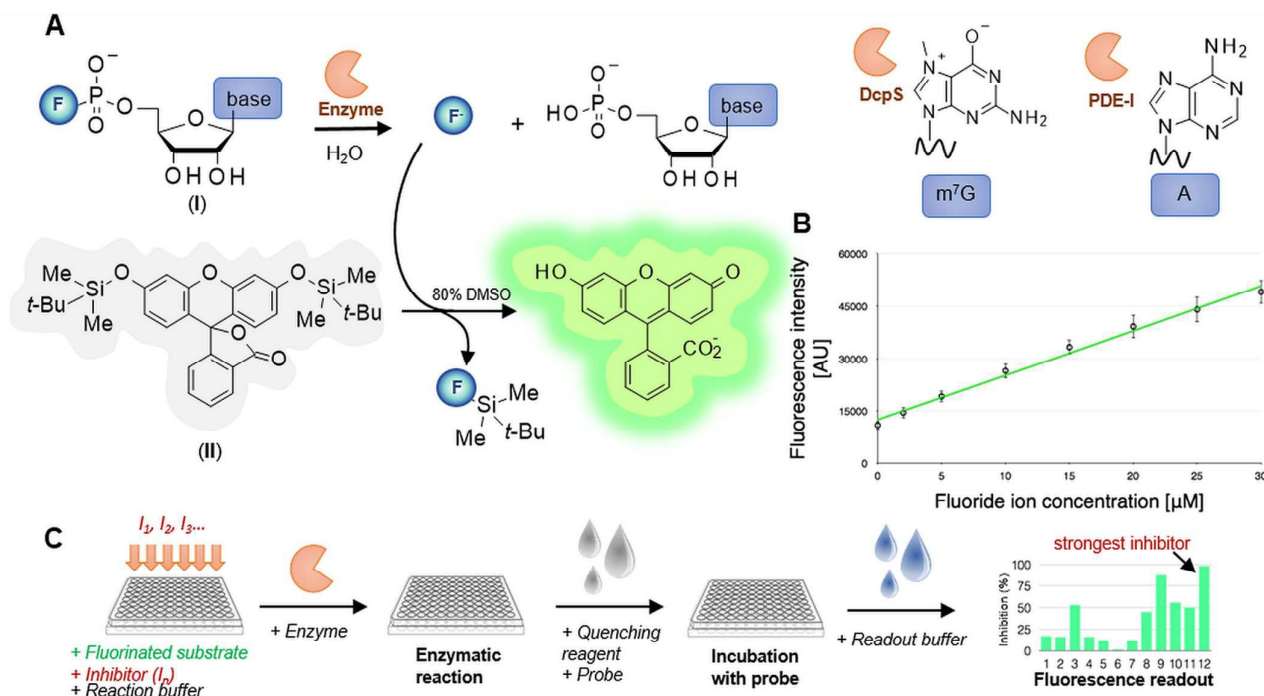


Fig. 1 A) General concept of the assay and the structures of substrates used for the enzymes DcpS and PDE-I. B) Typical dependence of fluorescein emission intensity on fluoride concentration (calibration curve from the DcpS assay). C) Assay flowchart.

in various aqueous samples, including samples from biological assays and living cells^{20–25} For our investigation, we chose two phosphohydrolases: a decapping scavenger pyrophosphatase (DcpS) and snake-venom phosphodiesterase I (PDE-I).

The scavenger decapping enzyme DcpS is a member of the HIT superfamily of phosphohydrolases and phosphotransferases that use a histidine triad for catalysis.²⁶ DcpS participates in mRNA degradation by hydrolysing the 7-methylguanosine-containing dinucleoside oligophosphates (5'-cap moieties) that are released after 3'-to-5' mRNA degradation.²⁷ DcpS might also play more general regulatory roles in gene expression, including regulation of mRNA splicing and miRNA stability.^{28–30} Notably, DcpS has also been identified as a molecular target in the treatment of spinal muscular atrophy (SMA), because DcpS inhibitors have been shown to improve motor function in two mouse SMA models.^{31–33} Although a few methods currently exist for identifying or characterising DcpS activity, inhibition and binding, including radioactive binding- and activity-based assays,^{27,31} HPLC assays,³⁴ fluorescence-quenching titration,³⁵ and covalent probes,³⁶ these methods are either time-consuming or require a specialised reagents and experimental setup. Thus, a straightforward and inexpensive HTS method to identify and evaluate potential DcpS inhibitors, based on readily available reagents, could expedite efforts to develop novel DcpS-targeting therapeutics.

PDE-I from *Crotalus adamanteus* venom is commonly used as a model enzyme for developing phosphodiesterase and pyrophosphatase assays. PDE-I is an oligonucleotide hydrolase

that releases nucleoside 5'-monophosphates from 3'-hydroxy ribo- and deoxyribo-oligonucleotides; this exonuclease can attack both DNA and RNA from their 3'-hydroxyl ends, but can also use nucleoside 5'-diphosphates and -triphosphates as substrates. PDE-I has been shown to hydrolyse various substrates such as ATP, cAMP, bis-*p*-nitrophenyl phosphate, and *p*-nitrophenyl ester of thymidine-5'-phosphate, but to exhibit negligible 5'-phosphatase-like activity.³⁷ In contrast to DcpS, PDE-I requires divalent cations for catalysis and is inhibited by EDTA. Therefore, we expected PDE-I to serve as a favourable model for determining the utility of our assay for divalent-cation-dependent enzymes.

The assay presented here was developed based on the reaction of fluoride ions with bis-(*tert*-butyldimethylsilyl)-fluorescein) (TBDMS-FL).²⁰ After thorough optimisation, we used the assay to screen a small library of 76 compounds, which mostly included various nucleotide derivatives. Selected compounds were further characterised to determine their IC_{50} values, verify the screening results, and assess the utility of the method.

Results and discussion

Design and optimisation of the screening assay

The general concept of the assay is shown in Fig. 1. The assay is based on two key reagents: a nucleoside 5'-fluoromonophosphate (NMPF; I) and a fluoride-sensitive

fluorogenic probe (in our case, TBDMS-FL; II). NMPF serves as an artificial substrate that is cleaved by the enzyme to release a fluoride ion and NMP. An appropriate NMPF was used for each enzyme: 7-methylguanosine 5'-fluorophosphate (m^7 GMPF) for

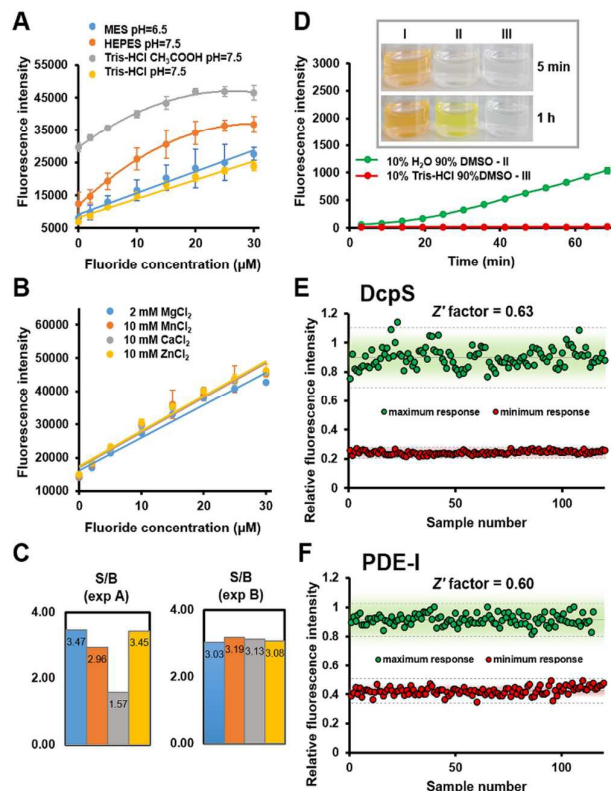


Fig. 2 Assay optimisation and validation. A) Calibration curves for fluoride samples dissolved in different buffers (averages from triplicate experiments); B) influence of various divalent cations on the calibration curve in Tris-HCl pH 7.5; C) max. signal (30 μ M) to background (0 μ M) ratios for curves shown in panels A (left) and B (right); D) stability of TBDMS-FL in different solutions at 30 $^{\circ}$ C: fluorescence changes over time (graph) and pictures of probe solutions in pure DMSO (I), DMSO:H₂O 9:1 (II) and DMSO:Tris-HCl (III) after 5 min and 1 h from preparation (inset); E) and F) Z' factor determination for hDcpS and PDE-I under optimised conditions.

DcpS and adenosine 5'-fluorophosphate (AMPF) for PDE-I. Importantly, all reagents were efficiently synthesised in only a few synthetic steps from commercially available starting materials (Figs. S1, S2). The fluoride released from NMPF upon enzymatic cleavage is quantified based on its chemical reaction with an organic-aqueous solution of TBDMS-FL, which leads to the formation of a fluorescent product (fluorescein, FL).²⁰ The sample is then mixed with a readout buffer and the emission intensity is measured. This fluorescence signal is directly proportional to the fluoride concentration (Fig. S3), and thus the fluorescence intensity should be diminished in the presence of strong inhibitors. Out of the several distinct fluorogenic probes reported in the literature,¹⁹ we selected TBDMS-FL because it was shown to be useful for quantifying fluorides in various samples, including water, toothpaste, and enzymatic reaction samples.^{20,21,38}

To optimise the assay and assure its reproducibility, we tested diverse reaction conditions for each enzyme, including

conditions of the enzymatic reaction (buffer composition, substrate and inhibitor concentrations, reaction time, metal ion additives) and the subsequent fluoride-detection reaction (probe solution preparation, DMSO content, reaction time and temperature). We found that the assay is compatible with a majority of buffers, including Tris-HCl, HEPES, and MES (Fig. 2). However, Tris buffers whose pH was >8 or which contained CH₃COOH produced high levels of fluorescence upon mixing with TBDMS-FL, even in the absence of fluorides, probably due to the chemical decomposition of the probe (Fig. S4). Among the tested reagents for quenching the enzymatic reaction, 30% acetonitrile and aqueous EDTA were found to be compatible with the probe, whereas strong acids (e.g. formic acid) prevented probe activation. Moreover, TBDMS-FL solution stability was found a crucial factor for assay reproducibility: In our hands, the probe was highly unstable in pure DMSO (with observable decomposition occurring within a few minutes), relatively more stable in a DMSO:water mixture (9:1 v/v), and most stable in a DMSO:Tris pH 7.6 (9:1) mixture (Fig. 2). We determined that a medium containing at least 80% DMSO is necessary for quantitative reaction of TBDMS-FL with fluoride what is in agreement with previously published studies.²¹ Lastly, we also investigated how Mg²⁺ and other divalent metal cations affect the reaction between fluoride ions and the fluorogenic probe (Fig. 2). The presence of 10 mM MgCl₂ in the enzymatic reaction mixture markedly decreased the slope and thus the signal-to-background ratio (S/B) of the fluorescence calibration curve, likely due to the low solubility of MgF₂ (Fig. 2). By contrast, CaCl₂, MnCl₂, and ZnCl₂ up to 10 mM and MgCl₂ up to 2 mM either did not affect the calibration curve or affected it only slightly (Fig. 2, S5, S6). Because Ca²⁺ supports PDE-I catalysis equally well as Mg²⁺, we selected it for further PDE-I assay development.³⁷ Overall, our results showed that whereas diverse conditions are compatible with the assay, certain factors are crucial for obtaining sufficiently high signal-to-background ratio and reproducibility. Our findings might explain why although fluoride-sensitive probes were successfully used to assay γ -butyrobetaine hydroxylase,²¹ other attempts to develop such assay were reported to be unsuccessful.³⁹ In Table S1, we present a summary of the most critical conclusions from our optimisation studies, which might facilitate the adaptation of our assay to other enzymes. To verify whether our method can be adapted to the HTS format, we determined the Z' factor for the reaction under the optimised conditions; Z' factor is a simple statistical parameter used in evaluating HTS assays and its value can theoretically range from $-\infty$ to 1.0, with values above 0.5 typically accepted as suitable for HTS.⁴⁰ The Z' value for each assay was estimated from 120 negative-control samples emulating complete inhibition of the enzyme and 120 positive-control samples (i.e. reactions performed up to 30% NMPF conversion in the absence of inhibitor). The optimised conditions for DcpS were 60 μ M m^7 GMPF and 25 nM DcpS in Tris-HCl, pH 7.6, containing 0.75 mg/mL BSA. Under these conditions, the K_M for m^7 GMPF was in the sub-nanomolar range (Fig. S7), and a 30% substrate conversion, which corresponded to 15 μ M fluoride and provided an adequate fluorescence response for the

competition assay, was achieved after approximately 55 min. The optimised conditions for PDE-I were 30 μ M AMPF and 0.08 μ g/mL enzyme, in 50 mM Tris-HCl, pH 7.5, containing 10 mM CaCl₂ and 0.75 mg/mL BSA. Under these conditions, a 30%

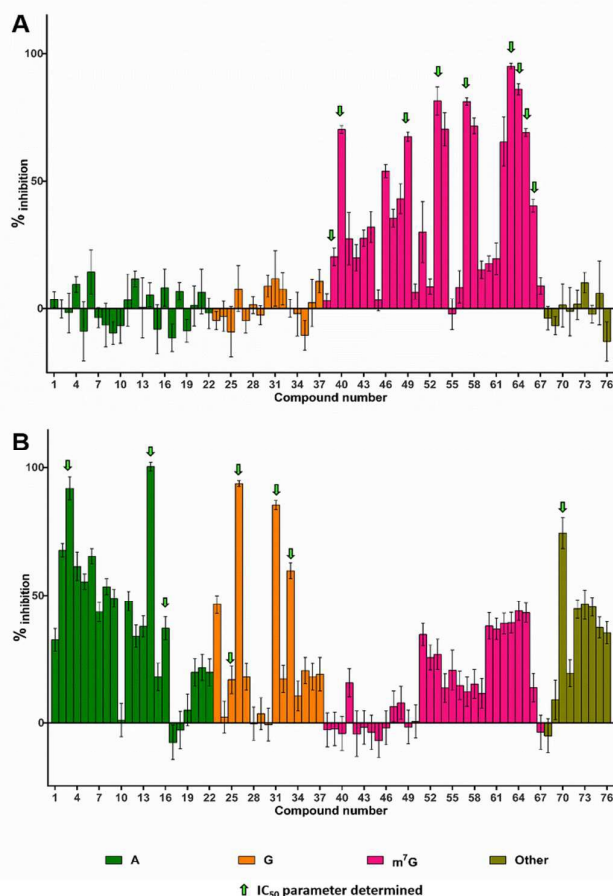


Fig. 3 Results of 76-compound library screening against DcpS (A) and PDE-I (B). The strongest inhibitors are characterised by the highest %inhibition. Table S2 shows the structures of the inhibitors together with the percentage of inhibition. Compounds selected for further evaluation are indicated by green arrows.

substrate conversion was achieved within 30 min, and this corresponded to the presence of 10 μ M fluoride. The Z' values estimated for the DcpS and PDE-I assays were 0.63 and 0.60, respectively, which indicated that these assays are suitable for inhibitor screening (Fig. 2).

Screening of a nucleotide library against DcpS and PDE-1

To verify the usefulness of our assay, we screened a small 'in-house' library of 76 compounds against DcpS and PDE-I. The library contained various small nucleotides as well as their analogues modified within the ribose moiety or phosphate chain. Among the compounds were several m⁷G nucleotides, which are analogues of the mRNA cap structure, the natural substrate for DcpS. The library also contained various A, G, C, and U nucleotides, including known PDE-I substrates, and certain unrelated compounds (such as folic acid; see Table S2 for complete library composition). This design of the library enabled straightforward verification of the screening results for DcpS and PDE-I based on the already-established

characteristics of these enzymes and also allowed new insights into their specificity to be gained.

The screening assays for both DcpS and PDE-I were performed under the optimised conditions described in the preceding subsection and in the presence of a tested inhibitor (used at 20 μ M). Because the fluorescence signal was directly proportional to the product concentration, the strongest inhibitors were characterised by the lowest fluorescence intensity. The percentage of inhibition (%_{inhib}) was calculated as the ratio of fluorescence signal loss in the presence of inhibitor to the signal in the absence of inhibitor as described in Experimental. The results are shown in Fig. 3.

The DcpS screening revealed several potential inhibitors, all from the pool of m⁷G derivatives. This agrees with the previous finding that DcpS is highly specific towards m⁷G nucleotides.³⁵ The compounds that received the highest percentage of inhibition included m⁷GDP (**40**, %_{inhib} = 70 %) and phosphate-modified analogues of the dinucleotide m⁷GpppG. m⁷GDP is a natural inhibitor of human DcpS (hDcpS) and its IC₅₀ was estimated to be 4.17 ± 0.50 μ M using an HPLC based assay and m⁷GpppG as substrate.³⁵ The dinucleotides that received highest percentage of inhibition were m⁷GpppG analogues carrying a boranophosphate moiety (i.e. an O-to-BH₃ substitution) at the β -position (%_{inhib} = 95 for **63** and 86 for **64**) and a methylenebisphosphonate (**53**; O-to-CH₂, %_{inhib} = 82) or imidodiphosphate (**57**; O-to-NH, %_{inhib} = 81) at the γ/β -position, and these have also been previously identified as cleavage-resistant, tight hDcpS binders.⁴¹⁻⁴³ Thus, we concluded that the screening results corresponded well with the known characteristics of hDcpS.

PDE-I screening also revealed several potential inhibitors, and most of these were from the pool of A and G nucleotides. Previous work has established that natural NTPs are not only substrates, but also weak inhibitors of PDE-I;³⁷ in agreement, the percentage of inhibition here for ATP (**1**) and its unhydrolysable analogue S_P-ATP α S (**3**) were 32% and 92%, respectively. Interestingly, the two nucleotides featuring the highest PDE-I percentage of inhibition were fluoromethylenebisphosphonate analogues of ADP and GDP (100% and 94% for ApCH₂pF – **14** and GpCH₂pF – **26**, respectively). These compounds represent a novel class of unhydrolysable nucleotide analogues recently described by our group,¹³ and the compounds have not been previously evaluated as enzyme inhibitors. The presence of an O-to-F substitution at the terminal phosphate appears to be crucial for inhibition, because, for example, the percentage of inhibition was markedly lower for GpCH₂p (**25**, %_{inhib} = 17%), the non-fluorinated counterpart of GpCH₂pF. Moreover, a high percentage of inhibition obtained for folic acid (**70**, %_{inhib} = 74%) identified this compound as another previously unknown potential inhibitor of PDE-I. Based on the screening results, two small sub-libraries of potential inhibitors of each enzyme were selected from the library for further evaluation.

IC₅₀ determination

Next, we used the same conditions as those in the initial screening and determined the selected compounds' IC₅₀ values

(i.e. the concentrations required to reduce the enzyme activity by half). A 10-point half-log dilution series was tested for each

compound, and the obtained fluorescence values were plotted against the logarithm of inhibitor concentration together with

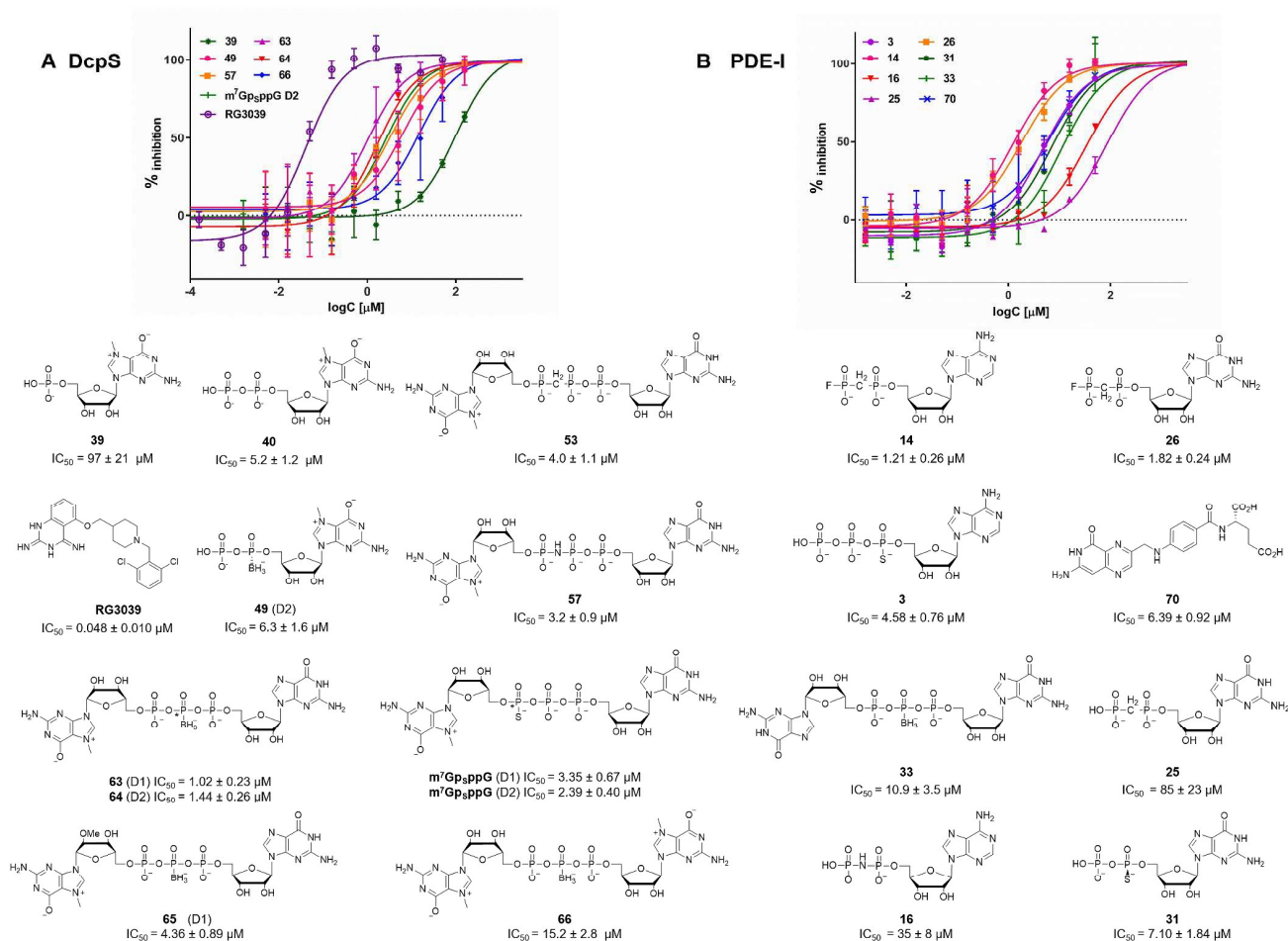


Fig. 4 Characterisation of compounds selected from the DcpS (A) and PDE-I (B) inhibitor-screening assays. The IC_{50} values were determined by plotting \log (inhibitor concentration) vs. response (%inhibition); standard errors of IC_{50} values were determined in QtiPlot. D1 and D2 refer to diastereomers of a given compound resulting from the presence of a stereogenic phosphorus atom (marked with *; D1 denotes always the faster migrating isomer on RP HPLC column).

zero and the maximal-response values. To determine the IC_{50} values, the data were fitted to the standard dose-response equation as described in Experimental.

For DcpS, we determined the IC_{50} for 9 mono- and dinucleotide mRNA cap analogues selected from the library, including the product (m^7GMP), the natural inhibitor (m^7GDP), and several phosphate-modified analogues of the substrate (m^7GpppG). Furthermore, we included 2 cap analogues (m^7GpppG D1 and D2) that were not present in the library but were previously found to be non-hydrolysable DcpS-binders,⁴⁴ and RG3039 – a previously described, quinazoline-based potent inhibitor of DcpS.³¹ For PDE-I, we evaluated 7 purine nucleotides and folic acid.

The results from multiple experiments for DcpS and PDE-I are summarised in Fig. 4 and Table S3. The determined IC_{50} values correlated well with the initial percentage of inhibition for both PDE-I and DcpS inhibitors. The DcpS results confirmed

that m^7GDP (**40**) is a low-micromolar inhibitor of DcpS ($IC_{50} = 5.2 \mu M$), as previously found in an HPLC-based study conducted using m^7GpppG as a substrate.³⁵ We further determined that m^7GMP (**39**) was a very weak inhibitor of hDcpS, which also agreed with the results of previous studies.³⁵ The IC_{50} values obtained for unhydrolysable analogues of m^7GpppG were all below $5 \mu M$, and the analogue m^7GpppG BH₃P G D1 (**63**) was the strongest nucleotide inhibitor ($IC_{50} = 1.0 \mu M$). RG3039 was over 20-fold more potent than **63**, with IC_{50} of 0.048 nM. Taking into account the differences in the assay design, this is in fair agreement with the values of 3-4 nM reported previously.^{31,33} For PDE-I, the results confirmed that the strongest inhibitors were two 5'-(2-fluoro-1,2-methylenediphosphate) nucleotide analogues (**14** and **26**; $IC_{50} < 2 \mu M$ for both). By contrast, all tested non-fluorinated nucleotide analogues, except ATP α S ($IC_{50} = 4.6 \mu M$), were poor inhibitors ($IC_{50} > 10 \mu M$). For folic acid, we measured an IC_{50} of

6.4 μM , which identified this compound as a non-nucleotide inhibitor of PDE-I.

Lastly, because unnatural substrates of the enzymes were used in our assay, we sought to verify whether the identified inhibitors would also be effective when a natural substrate was

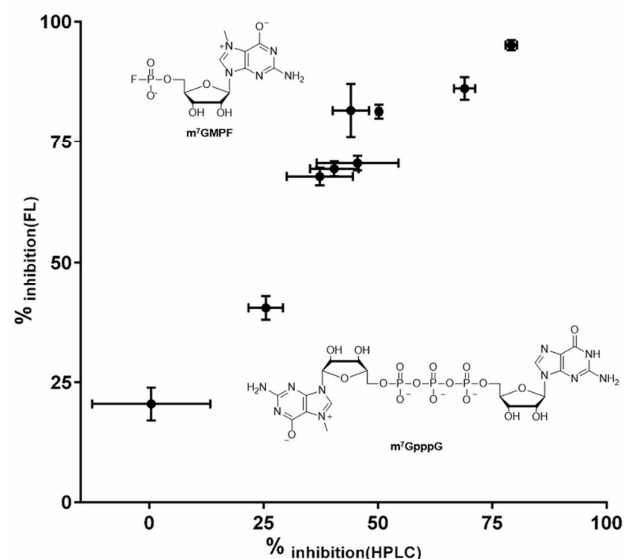


Fig. 5 Correlation between the results from fluorescence-based hDcpS screening performed using $m^7\text{GMPF}$ as a substrate and HPLC-based hDcpS screening by using $m^7\text{GpppG}$ as a substrate for 9 selected compounds. In both assays, we used 60 μM substrate and 20 μM inhibitors. The reaction was stopped at a time point corresponding to 25% substrate conversion in the reaction without inhibitor. The data points are averages from 3 experiments \pm S.D.

used. Thus, we additionally evaluated a set of 9 selected DcpS inhibitors in an HPLC-based screening by using the natural substrate, $m^7\text{GpppG}$. We found that the HPLC-based screening scores correlated well with the fluorescence-assay screening scores for all inhibitors (Fig. 5 and Table S4). This indicates that the use of $m^7\text{GMPF}$ instead of the natural substrate does not distort the screening results for DcpS. Collectively, our results confirm that the assay developed in this study is a useful tool for rapid characterisation of putative inhibitors of phosphohydrolases and determination of their IC_{50} values is 10 times faster than standard HPLC method.

Conclusions

Certain nucleotide-specific phosphohydrolases can cleave P-F bonds in the fluorophosphate analogues of nucleotides to release a fluoride ion. In this study, we harnessed this P-F bond cleavage reaction to develop an enzymatic assay for phosphohydrolases. We achieved this by using a molecular sensor (a TDBMS-FL fluorogenic probe) that quantitatively reacts with fluoride ions to release a fluorescent product (fluorescein). The assay conditions were successfully optimised for two model enzymes, the pyrophosphatase DcpS and the nuclease PDE-I, and the assay utility was demonstrated by screening the enzymes against a small library of nucleotide derivatives. Based on the screening results, several potential

inhibitors were selected and their IC_{50} values were determined using the same methodology, which identified compounds that inhibited the enzymes in the sub-millimolar to low-micromolar range. These results confirmed the utility of the assay for evaluating potential inhibitors of both metal-dependent (PDE-I) and metal-independent (hDcpS) phosphohydrolases. Notably, our assay is the first nonradioactive and HTS-amenable assay for assessing potential inhibitors of hDcpS. The enzyme DcpS plays a complex and incompletely understood role in mRNA quality control,^{30,45} and detailed profiling of DcpS specificity might be a key to deciphering the link between DcpS enzymatic activity and its other functions, and could lead to the discovery of useful tools for further studies. Furthermore, compounds that exert inhibitory effects on DcpS are also potential therapeutics for SMA.^{31,32} Both of these areas of DcpS-related research might be efficiently supported by our HTS assay, which is a useful alternative to previously described radioactive or low-throughput assays.

The broad range of conditions compatible with our assay and the several optimisation possibilities suggest potential wider applicability of the assay in the future. First, the synthetic availability of NMPF enables easy adaptation of the assay to enzymes that exhibit distinct nucleotide specificities. The assay should be particularly useful for screening other HIT superfamily enzymes. These enzymes differ in their biological role and in specificity towards nucleotide-derived substrates, but all play key roles in the regulation of gene expression, and, consequently, several of the enzymes have been linked to disease development.⁴⁶ For example, human Fhit is an Ap_nA hydrolase that functions as a tumour suppressor,⁴⁷ and aprataxin functions in single-stranded DNA repair and has been associated with ataxia-ocular apraxia.^{48,49} Second, the assay can also be tailored to specific applications by altering the structure of the fluoride-specific molecular sensor. The recent efforts devoted towards developing fluoride-sensitive probes that can work even under completely aqueous conditions^{23,50,51} could open the possibility for online monitoring of P-F bond enzymatic cleavage. We are currently investigating the applicability of the assay for other HIT superfamily enzymes and evaluating fluoride sensors featuring properties distinct from those of TBDMS-FL.

Experimental

Preparation of enzymatic substrate solutions ($m^7\text{GMPF}$ and AMPF)

The substrate nucleotides were synthesised as previously described,¹³ and purified using ion-exchange chromatography (DEAE Sephadex A-25) followed by RP-HPLC and then isolated as ammonium (NH_4^+) salts after repeated freeze-drying. The ~ 5 mM stock solution of $m^7\text{GMPF}$ was prepared by dissolving 10 mg of the compounds in 5 mL of deionised water. The exact concentration was adjusted by measuring optical density at 260 nm in phosphate buffer pH 6 and using an extinction coefficient (ϵ_{260}) of $11400 \text{ M}^{-1} \text{ cm}^{-1}$. The ~ 5 mM stock solution of AMPF was prepared by dissolving 7 mg of the compounds in

4 mL of deionised water. The exact concentration was adjusted by measuring optical density at 260 nm in phosphate buffer pH 7 by using $\epsilon_{260} 15020 \text{ M}^{-1} \text{ cm}^{-1}$.

Synthesis of the fluorogenic probe FTBS

The fluorogenic probe, fluorescein di-*tert*-butyldimethylsilyl ether (TBDMS-FL), was synthesised as previously described.²⁰ We mixed fluorescein (800 mg, 2.41 mmol) and imidazolide (860 mg, 12.60 mmol) in anhydrous DMF (8.5 mL), and to this solution, added *tert*-butyldimethylsilyl chloride (1.40 g, 9.30 mmol). After the reaction mixture was stirred for 12 h at room temperature, the resultant solution was poured into saturated brine (~60 mL) and extracted with ethyl acetate. The combined organic extracts were washed with saturated brine and dried over anhydrous MgSO_4 , and the solvent was evaporated to dryness. The product was purified using flash chromatography (Reveleris® Prep Purification System, Reveleris® Silica 12 g column, linear 0%–30% gradient of ethyl acetate in hexane) and, after evaporation, was isolated as a white solid (617 mg, 46%).

Preparation of FTBS solution

The probe solution was freshly prepared before each screening assay. FTBS (3.0 mg, 5.36 μmol) was dissolved in 50 μL of ethyl acetate and the solution was diluted in 10 mL of 9:1 (v/v) mixture of DMSO and aqueous Tris buffer (50 mM Tris-HCl, pH 7.60, 0.5 mM EDTA, 200 mM KCl) to a final FTBS concentration of 5.3 μM . We found that in a 9:1 DMSO:Tris mixture, the probe was more stable than in pure DMSO or 9:1 DMSO:water. The prepared FTBS solution was stored at room temperature and was stable for at least 1 h.

Enzymes

PDE-I from *C. adamanteus* (E.C. 3.1.4.1) venom was purchased as a lyophilised solid from Sigma-Aldrich. The solid was dissolved in a storage buffer (110 mM Tris-HCl, pH 8.9, 110 mM NaCl, 15 mM MgCl_2 , 50% glycerol) to prepare a 1 mg/mL solution and then stored at -20°C . Before the assay, the enzyme was diluted to 2.5 $\mu\text{g/mL}$ with PDE-I buffer (buffer composition is listed under 'Inhibitor-screening assay').

Human DcpS was expressed as previously described, with minor modifications.⁵² The concentration of the protein was determined spectrophotometrically by assuming $\epsilon_{280} = 30400 \text{ M}^{-1} \text{ cm}^{-1}$. The enzyme was stored at -80°C in a storage buffer (50 mM Tris-HCl, pH 7.6, 200 mM NaCl, 1 mM DTT, 10% glycerol).

Compound library

The library included 76 compounds, each of which was dissolved in deionised water at 5 mM and stored at -80°C . Table S2 lists the compound structures and references to their sources. For the purpose of screening experiments, the master plate was copied to secondary plates containing the compounds dissolved in deionised water at 0.5 mM. The stock solution of RG 3039 (DC Chemicals) was obtained by dissolving the compound at 5 mM in DMSO.

Inhibitor-screening assay

Enzymatic assays were performed in 96-well, black, non-binding assay plates. Each well contained an appropriate substrate (nucleoside fluorophosphate) and the tested inhibitor in an appropriate buffer, and the total volume of the

reaction mixture was 200 μL . The reaction components were preincubated for 10–15 min at 30°C and then the enzyme was added. In the blank (control) reactions, the inhibitor was replaced with water; the controls were run in triplicates. The remaining 16 wells in each plate were used for preparing the calibration curve; they contained increasing concentrations of fluoride (0–30 μM) in the reaction buffer.

Samples were incubated with the enzyme at 30°C until 25%–30% substrate conversion was achieved (the reaction time for each enzyme was predetermined by time-dependent HPLC measurements), following which the reactions were quenched by mixing with 100 μL of the quenching reagent and aliquots (25 μL) were transferred into a new plate. Next, 90 μL of the fluorogenic probe solution was added to each well and the samples were incubated for 60 min at 30°C , and, lastly, 100 μL of HEPES buffer (200 mM, pH 7.0) was added and the fluorescence was measured using a microplate reader (Tecan Infinite 200PRO, $\lambda_{\text{ex}} = 480 \text{ nm}$, $\lambda_{\text{em}} = 535 \text{ nm}$, excitation bandwidth = 9 nm, emission bandwidth = 20 nm).

Specific conditions:

PDE-I assay: PDE-I buffer, 30 μM AMPF, 6.5 μL of PDE-I (2.5 $\mu\text{g/mL}$), 20 μM inhibitor; reaction time, 30 min; quenching solution, 5 mM aqueous EDTA, pH adjusted to 7.0 with NaOH.

PDE-I buffer: 50 mM Tris-HCl, pH 7.5, 10 mM CaCl_2 , 0.75 mg/mL BSA.

DcpS assay: DcpS buffer, 60 μM m^7GMPF as a substrate, 25 nM DcpS enzyme, 20 μM inhibitor; reaction time, 55 min; quenching solution, acetonitrile.

DcpS buffer: 50 mM Tris-HCl, 200 mM KCl, 0.5 mM EDTA, 0.75 mg/mL BSA.

The screening results were quantified by calculating percentage of inhibition ($\%_{\text{inhib}}$), which was defined as following:

$$\%_{\text{inhib}} = \frac{F_{\text{cont}} - F_{\text{inhib}}}{F_{\text{cont}} - F_{\text{bg}}} * 100\%$$

where F_{cont} indicates the average fluorescence readout from control reactions (without inhibitor). F_{inhib} indicates the fluorescence readout from reaction with the given inhibitor. F_{bg} indicates the background fluorescence (sample from the calibration curve containing 0 μM of fluoride).

IC₅₀ determination

The IC₅₀ experiments were conducted in the same manner in which the initial screening was performed, except that instead of a single concentration of each inhibitor, a 10-point half-log dilution series (starting at 158 μM or 50 μM for DcpS and PDE-I, respectively) was tested. The experiments were run in triplicates. To determine the IC₅₀ values, the data were fitted to the standard dose-response equation:

$$y = A_1 + \frac{A_2 - A_1}{1 + 10^{x - \log_{10} \text{IC}_{50}}}$$

where A_1 is bottom asymptote, A_2 is top asymptote, x is inhibitor concentration in logarithmic scale, and y is $\%_{\text{inhib}}$.

Z' determination

The performance of the HTS assays was evaluated by determining the Z' factor.⁴⁰ The measurements were

performed in 96-well, black, non-binding assay plates. An appropriate substrate (nucleoside fluorophosphate) in 200 μL of assay buffer (hDcpS or PDE-I) was added to each well, and then to columns 1–5, the stopping reagent was added. Next, the 96-well assay plates were incubated for 10–15 min at 30 $^{\circ}\text{C}$ and then the enzyme was added into all wells. After incubation for a period of time necessary to achieve 25–30% substrate conversion (see below), the enzymatic reactions in columns 6–10 were stopped by adding the stopping reagent. The remaining 16 wells were used for calibration; they contained increasing concentrations of fluoride (0–30 μM) in the reaction buffer.

PDE-I Z' determination: PDE-I buffer, 30 μM AMPF, 6.5 μL of PDE-I (2.5 $\mu\text{g}/\text{mL}$); incubation time, 30 min; quenching solution, 5 mM aqueous EDTA, pH adjusted to 7.0 with NaOH.

DcpS Z' determination: DcpS buffer, 60 μM m⁷GMPF as a substrate, 25 nM DcpS enzyme; incubation time, 55 min; quenching solution, 100% acetonitrile.

Determination of kinetic constants for m⁷GMPF

In order to determine kinetic parameters for m⁷GMPF as human DcpS substrate enzymatic reactions were performed in 50 mM Tris-HCl buffer (pH 7.6) containing 200 mM KCl, 0.5 mM EDTA in the total volume of 1200 μL at 20 $^{\circ}\text{C}$ (at higher temperatures the K_{M} value was below 1 μM , thus below the range of our detection method). The initial substrate concentration ranged from 0.5 μM to 50 μM and used enzyme concentration was 1.7 nM. Reactions were quenched by addition 50 μL of HCOOH to 100 μL aliquots taken from the reaction mixtures at different time points (1, 3, 5, 7, 10, 15, 20 min). The samples were analyzed by reversed-phase HPLC (Agilent Technologies 1200 Series, Santa Clara, CA, USA) with applied analytical column (Supelcosil LC-18-T column, 4.6 mm \times 250 mm, 5 μm). During analysis column was eluted with a linear gradient (15 min; flow rate, 1.3 ml/min) of 0–50% methanol in aqueous 0.1 M KH_2PO_4 . The product concentration was determined by analysing the fluorescence signal at 370 nm (excitation 260 nm). The initial velocity of m⁷GMPF hydrolysis was calculated by linear regression of the product concentration versus time. The initial velocities were plotted against substrate concentration and K_{M} and V_{max} parameters were determined from hyperbolic fits to the Michaelis–Menten equation by nonlinear regression using GraphPad Prism software.

Acknowledgements

We thank Prof Mike Kiledjian (Rutgers University) for the plasmid encoding hDcpS, Marcin Warminski (University of Warsaw) for expressing and purifying the hDcpS protein, and Dr Anna Rydzik (Ludwig-Maximilians-Universität München) for useful advice on setting up the assay. We are also grateful to all members of the Laboratory of Bioorganic Chemistry, University of Warsaw, who provided compounds for the nucleotide library. Financial support from the National Centre for Research and Development (Grant No LIDER 003/L-5/2013 to J.K.), the National Science Centre, Poland (Grant No UMO-

2012/05/E/ST5/03893 to J.J.), and Ministry of Science and Higher Education (Grant No DI2013 014943 to M.R.B.) is gratefully acknowledged.

Notes and references

1. M. Idzko, D. Ferrari and H. K. Eltzschig, *Nature*, 2014, **509**, 310–317.
2. H. Zimmermann, M. Zebisch and N. Straeter, *Purienerg. Signal.*, 2012, **8**, 437–502.
3. H. K. Eltzschig, M. V. Sitkovsky and S. C. Robson, *New Eng. J. Med.*, 2012, **367**, 2322–2333.
4. J. R. Penades, J. Donderis, M. Garcia-Caballer, M. Angeles Tormo-Mas and A. Marina, *Curr. Opin. Microbiol.*, 2013, **16**, 163–170.
5. S. H. Francis, M. A. Blount and J. D. Corbin, *Physiol. Rev.*, 2011, **91**, 651–690.
6. C. T. Rampazzo, Maria Grazia. Jordheim, Lars Petter, *Cancer Chemoth. Pharm.*, 2015, 1–11.
7. S. M. Hacker, N. Hardt, A. Buntru, D. Pagliarini, M. Moeckel, T. U. Mayer, M. Scheffner, C. R. Hauck and A. Marx, *Chemical Science*, 2013, **4**, 1588–1596.
8. S. M. Hacker, C. Hintze, A. Marx and M. Drescher, *Chem. Commun.*, 2014, **50**, 7262–7264.
9. S. M. Hacker, A. Buntz, A. Zumbusch and A. Marx, *ACS Chem. Biol.*, 2015, **10**, 2544–2552.
10. N. Hardt, S. M. Hacker and A. Marx, *Org. Biomol. Chem.*, 2013, **11**, 8298–8305.
11. M. Bollmark and J. Stawinski, *Nucleos. Nucleot.*, 1998, **17**, 663–680.
12. M. F. Aldersley, P. C. Joshi, H. M. Schwartz and A. J. Kirby, *Tetrahedron Lett.*, 2014, **55**, 1464–1466.
13. M. R. Baranowski, A. Nowicka, A. M. Rydzik, M. Warminski, R. Kasprzyk, B. A. Wojtczak, J. Wojcik, T. D. W. Claridge, J. Kowalska and J. Jemielity, *J. Org. Chem.*, 2015, **80**, 3982–3997.
14. M. F. Aldersley, P. C. Joshi, E. L. Ott, S. A. McCallum and A. J. Kirby, *Tetrahedron Lett.*, 2015, **56**, 5272–5274.
15. A. Guranowski, A. M. Wojdyla, M. Pietrowska-Borek, P. Bieganowski, E. N. Khurs, M. J. Cliff, G. M. Blackburn, D. Blaziak and W. J. Stec, *FEBS Lett.*, 2008, **582**, 3152–3158.
16. A. Guranowski, A. M. Wojdyla, J. Zimny, A. Wypijewska, J. Kowalska, M. Lukaszewicz, J. Jemielity, E. Darzynkiewicz, A. Jagiello and P. Bieganowski, *New J. Chem.*, 2010, **34**, 888–893.
17. K. Misiura, M. Bollmark, J. Stawinski and W. J. Stec, *Chem. Commun.*, 1999, 2115–2116.
18. A. L. Simonian, J. K. Grimsley, A. W. Flounders, J. S. Schoeniger, T. C. Cheng, J. J. DeFrank and J. R. Wild, *Anal. Chim. Acta*, 2001, **442**, 15–23.
19. M. Cametti and K. Rissanen, *Chem. Commun.*, 2009, 2809–2829.
20. X.-F. Yang, S.-J. Ye, Q. Bai and X.-Q. Wang, *J. Fluoresc.*, 2007, **17**, 81–87.
21. A. M. Rydzik, I. K. H. Leung, G. T. Kochan, A. Thalhammer, U. Oppermann, T. D. W. Claridge and C. J. Schofield, *Chembiochem*, 2012, **13**, 1559–1563.
22. A. M. Rydzik, R. Chowdhury, G. T. Kochan, S. T. Williams, M. A. McDonough, A. Kawamura and C. J. Schofield, *Chemical Science*, 2014, **5**, 1765–1771.

23. B. Ke, W. Chen, N. Ni, Y. Cheng, C. Dai, H. Dinh and B. Wang, *Chem. Commun.*, 2013, **49**, 2494-2496.
24. G. Sivaraman and D. Chellappa, *J. Mater. Chem. B*, 2013, **1**, 5768-5772.
25. S. Y. Kim, J. Park, M. Koh, S. B. Park and J.-I. Hong, *Chem. Commun.*, 2009, 4735-4737.
26. Brenner, C. 2014. Histidine Triad (HIT) Superfamily. eLS.
27. H. D. Liu, N. D. Rodgers, X. Jiao and M. Kiledjian, *EMBO J.*, 2002, **21**, 4699-4708.
28. O. Meziane, S. Piquet, G. D. Bosse, D. Gagne, E. Paquet, C. Robert, M. A. Tones and M. J. Simard, *Scientific Reports*, 2015, **5**.
29. V. Shen, H. Liu, S.-W. Liu, X. Jiao and M. Kiledjian, *RNA*, 2008, **14**, 1132-1142.
30. M. Zhou, S. Bail, H. L. Plasterer, J. Rusche and M. Kiledjian, *RNA*, 2015, **21**, 1306-1312.
31. J. Singh, M. Salcius, S. W. Liu, B. L. Staker, R. Mishra, J. Thurmond, G. Michaud, D. R. Mattoon, J. Printen, J. Christensen, J. M. Bjornsson, B. A. Pollok, M. Kiledjian, L. Stewart, J. Jarecki and M. E. Gurney, *ACS Chem. Biol.*, 2008, **3**, 711-722.
32. R. G. Gogliotti, H. Cardona, J. Singh, S. Bail, C. Emery, N. Kuntz, M. Jorgensen, M. Durens, B. Xia, C. Barlow, C. R. Heier, H. L. Plasterer, V. Jacques, M. Kiledjian, J. Jarecki, J. Rusche and C. J. DiDonato, *Hum. Mol. Genet.*, 2013, **22**, 4084-4101.
33. J. P. Van Meerbeke, R. M. Gibbs, H. L. Plasterer, W. Miao, Z. Feng, M.-Y. Lin, A. A. Rucki, C. D. Wee, B. Xia, S. Sharma, V. Jacques, D. K. Li, L. Pellizzoni, J. R. Rusche, C.-P. Ko and C. J. Sumner, *Hum. Mol. Genet.*, 2013, **22**, 4074-4083.
34. A. Wypijewska, E. Bojarska, J. Stepinski, M. Jankowska-Anyszka, J. Jemielity, R. E. Davis and E. Darzynkiewicz, *FEBS J.*, 2010, **277**, 3003-3013.
35. A. Wypijewska, E. Bojarska, M. Lukaszewicz, J. Stepinski, J. Jemielity, R. E. Davis and E. Darzynkiewicz, *Biochemistry*, 2012, **51**, 8003-8013.
36. E. C. Hett, H. Xu, K. F. Geoghegan, A. Gopalsamy, R. E. Kyne, Jr., C. A. Menard, A. Narayanan, M. D. Parikh, S. Liu, L. Roberts, R. P. Robinson, M. A. Tones and L. H. Jones, *ACS Chem. Biol.*, 2015, **10**, 1094-1098.
37. S. S. M. Al-Saleh and S. Khan, *Prep. Biochem. Biotech.*, 2011, **41**, 262-277.
38. X. Cheng, H. Jia, J. Feng, J. Qin and Z. Li, *Sensors Actuat. B-Chem.*, 2014, **199**, 54-61.
39. M. Yevglevskis, G. L. Lee, J. Sun, S. Zhou, X. Sun, G. Kociok-Kohn, T. D. James, T. J. Woodman and M. D. Lloyd, *Org. Biomol. Chem.*, 2016, **14**, 612-622.
40. J. H. Zhang, T. D. Y. Chung and K. R. Oldenburg, *J. Biomol. Screen.*, 1999, **4**, 67-73.
41. J. Kowalska, A. Wypijewska del Nogal, Z. M. Darzynkiewicz, J. Buck, C. Nicola, A. N. Kuhn, M. Lukaszewicz, J. Zuberek, M. Strenkowska, M. Ziemniak, M. Maciejczyk, E. Bojarska, R. E. Rhoads, E. Darzynkiewicz, U. Sahin and J. Jemielity, *Nucleic Acids Res.*, 2014, **42**, 10245-10264.
42. A. M. Rydzik, M. Kulis, M. Lukaszewicz, J. Kowalska, J. Zuberek, Z. M. Darzynkiewicz, E. Darzynkiewicz and J. Jemielity, *Bioorg. Med. Chem.*, 2012, **20**, 1699-1710.
43. M. Kalek, J. Jemielity, Z. M. Darzynkiewicz, E. Bojarska, J. Stepinski, R. Stolarski, R. E. Davis and E. Darzynkiewicz, *Bioorg. Med. Chem.*, 2006, **14**, 3223-3230.
44. J. Kowalska, M. Lewdorowicz, J. Zuberek, E. Grudzien-Nogalska, E. Bojarska, J. Stepinski, R. E. Rhoads, E. Darzynkiewicz, R. E. Davis and J. Jemielity, *RNA*, 2008, **14**, 1119-1131.
45. J. Martin, M. V. St-Pierre and J.-F. Dufour, *BBA-Bioenergetics*, 2011, **1807**, 626-632.
46. M. I. Hassan, A. Naiyer and F. Ahmad, *J. Cancer Res. Clin.*, 2010, **136**, 333-350.
47. L. D. Barnes, P. N. Garrison, Z. Siphshvili, A. Guranowski, A. K. Robinson, S. W. Ingram, C. M. Croce, M. Ohta and F. Huebner, *Biochemistry*, 1996, **35**, 11529-11535.
48. P. Tumbale, J. S. Williams, M. J. Schellenberg, T. A. Kunkel and R. S. Williams, *Nature*, 2014, **506**, 111+.
49. I. Ahel, U. Rass, S. F. El-Khamisy, S. Katyal, P. M. Clements, P. J. McKinnon, K. W. Caldecott and S. C. West, *Nature*, 2006, **443**, 713-716.
50. R. Hu, J. Feng, D. Hu, S. Wang, S. Li, Y. Li and G. Yang, *Angew. Chem. Int. Edit.*, 2010, **49**, 4915-4918.
51. S. Y. Kim and J.-I. Hong, *Org. Lett.*, 2007, **9**, 3109-3112.
52. A. M. Rydzik, M. Lukaszewicz, J. Zuberek, J. Kowalska, Z. M. Darzynkiewicz, E. Darzynkiewicz and J. Jemielity, *Org. Biomol. Chem.*, 2009, **7**, 4763-4776.